Oxidation Changes Physical Properties of Phospholipid Bilayers: Fluorescence Spectroscopy and Molecular Simulations

Lenka Beranova[1], Lukasz Cwiklik[1,2], Piotr Jurkiewicz[1], Martin Hof[1,*], Pavel Jungwirth[2,*]

J. Heyrovský Institute of Physical Chemistry, Academy of Sciences of the Czech Republic, v. v. i., Dolejškova 3, 18223 Prague 8, and Institute of Organic Chemistry and Biochemistry, Academy of Sciences of the Czech Republic and Center for Biomolecules and Complex Molecular Systems, Flemingovo nám. 2, 16610 Prague 6, Czech Republic

[*] Corresponding authors.

E-mails: martin.hof@jh-inst.cas.cz and pavel.jungwirth@uochb.cas.cz

[1] J. Heyrovský Institute of Physical Chemistry

[2] Institute of Organic Chemistry and Biochemistry

Abstract

Physical properties of oxidized phospholipid (OxPL) membranes consisting of binary mixtures of 1-palmitoyl-2-oleoyl-sn-glycero-3-phosphocholine (POPC) and 10 % of one of two OxPLs - 1-palmitoyl-2-glutaryl-sn-glycero-3-phosphocholine (PGPC) or 1-palmitoyl-2-(5'-oxo-valeroyl)-sn-glycero-3-phosphocholine (POVPC), were investigated experimentally and computationally. Fluorescence solvent relaxation (SR) and fluorescence correlation spectroscopy z-scan (FCS z-scan) show increased headgroup hydration and dynamics, and faster lateral diffusion in POPC membrane upon addition of OxPLs. The magnitudes of both effects are distinct for each of the two OxPLs. Molecular dynamics simulations corroborate the experimental findings providing at the same time a detailed molecular interpretation in terms of changes in phospholipid structure and orientation.

Introduction

OxPLs, which are oxidation products of polyunsaturated phospholipids [1], are involved in pathogenesis of atherosclerosis [2, 3], cancer [4], Alzheimer [5], and other diseases [6]. The molecular mechanisms of their action, however, remain unclear. PGPC and POVPC that were identified as critical markers of atherosclerotic progression [2, 7], are among the most physiologically active OxPLs. The two molecules differ only in groups terminating their truncated sn-2 chains (carboxyl in case of PGPC and aldehyde in POVPC; see Figure 1), however their biological functions were found to be distinct [8,9]. It was shown that POVPC binds to human macrophages via the platelet-activating factor receptor (PAF-R), but not all of the PAF-R stimulated genes are affected [10]. This suggests that POVPC regulatory function is also realized by alteration of physical properties of cellular membranes.

The conical shape of the truncated OxPLs and the presence of the polar groups at their sn-2 chains can promote positive membrane curvature [11] or lead to partial interdigitation [12] or even cell disintegration [13]. The structure of OxPL-containing bilayer can be partially deduced from its biological activity, i.e., since the sn-2 acyl chains of OxPLs are accessible to phospholipase A_2 [14] or macrophage scavenger receptor CD36 [15] their orientation is likely reversed protruding from the plasma membrane. This effect was studied experimentally [15, 16] and computationally [17, 18, 19].

Dynamics of oxidized phospholipid membranes has been measured using fluorescence anisotropy. Unfortunately, the obtained results are contradictory [12]. Fluorescence recovery after photobleaching applied to sperm plasma membranes was not sensitive enough to capture any changes in lipid lateral diffusion upon oxidation [20]. Here we investigate physical properties of binary lipid mixtures of POPC with either PGPC or POVPC. Phospholipid headgroup dynamics and hydration were assessed using SR method, while lateral diffusion of

a fluorescence lipid analog in planar supported phospholipid bilayers (SPBs) was measured using FCS z-scan technique. Measurements were complemented by molecular dynamics simulations of the same systems aimed at capturing at a detailed atomistic level structural and dynamical changes induced in the membrane by the presence of OxPLs.

Materials and Methods

Experimental

POPC, PGPC, POVPC were purchased from Avanti Polar Lipids, Inc. (Alabaster, AL) and Laurdan and Bodipy C_{12}-HPC (2-(4,4-difluoro-5,7-dimethyl-4-bora-3a,4a-diaza-s-indacene-3-dodecanoyl)-1-hexadecanoyl-sn-glycero-3-phosphocholine) fluorescent dyes from Invitrogen (Eugene, OR). The structures of lipids and fluorescent dyes are shown in Fig. 1.

SR experiments were performed on extruded large unilamellar vesicles (1 mM lipid) labeled with 1 mol% of Laurdan and suspended in 10 mM Hepes, pH = 7.4 and 150 mM NaCl. Laurdan is precisely located in the lipid bilayer at the level of sn-1 carbonyl [21] and the recorded time-dependent Stokes shift correlates to headgroup hydration and mobility [22].

FCS z-scan was used to study lateral diffusion of Bodipy C_{12}-HPC, in SPB's. For detailed description of the method and its possible application please see [23].

The methodology of both experimental techniques, including sample preparation, was identical to the previously described one [24], except that the SPBs were formed on the bottom glass of LabTek slides (Thermo Fisher Scientific, Waltham).

Computational

In MD simulations, performed using the Gromacs program package [25], the united-atom Berger force field was employed for both lipid and oxPLs molecules [17, 26], and combined with the SPC model for water [27]. Simulations were performed for a periodic box

containing 128 lipid molecules and 4476 molecules of water. The initial size of the unit cell was equal to 6.5×6.5×7.1 nm^3. The constant pressure and temperature canonical ensemble was employed with the pressure of 1 bar controlled using a semi-isotropic Parrinello-Rahman barostat [28], and the temperature of 310 K imposed by a Nose-Hoover thermostat [29]. A cutoff of 1 nm was used for non-bonded interactions, with the Particle-Mesh-Ewald algorithm accounting for long-range electrostatic forces [30]. A timestep of 2 fs was employed and 100 ns trajectories were collected. Simulations were started by exchanging 14 randomly chosen POPC molecules (7 in each leaflet) in the previously equilibrated pure POPC bilayer with either PGPC or POVPC molecules. First 50 ns of each trajectory were treated as equilibration and were omitted from the analysis.

Results and discussion

Experiment

SR results for Laurdan, reflecting hydration and mobility at the sn-1 carbonyl groups of the bilayer, are summarized in Table 1. The total spectral shift, $\Delta\nu$, proportional to headgroup hydration, increased upon addition of both OxPLs (evident in particular at 5°C), with the membrane containing POVPC being considerably more hydrated than that with PGPC. Local mobility was even more affected by the presence of OxPLs. Also in this case, the observed shortening of relaxation time, τ_r, was larger for POVPC than for PGPC containing bilayer. The more hydrated and mobile Laurdan microenvironment likely results from the presence of OxPL short sn-2 chains, which may introduce free space below the glycerol level facilitating water penetration and reorientation of hydrated lipid moieties (water at this level is fully constrained by the lipids). But the obtained results are not only due to the effect of chain truncation. Comparison of the two OxPLs clearly shows that change of the functional group terminating the oxidized chain significantly affects the measured parameters.

Thus, the different biological functions [8,9] and cell location [7] of PGPC and POVPC can be due to not only specific receptor recognition, but also distinct physical properties PGPC- and POVPC-containing membranes.

Z-scan FCS measurements of lateral diffusion of a fluorescent lipid analog (Bodipy C_{12}-HPC) provide the following mean diffusion coefficients: D_{POPC} = (4.17 ± 0.06) ms, $D_{10\%\ PGPC}$ = (4.55 ± 0.14) ms, and $D_{10\%POVPC}$ = (4.37 ± 0.08) ms. The faster lateral diffusion in both oxPL-containing bilayers pairs well with elevated headgroup fluidity probed by Laurdan. The differences between PGPC and POVPC in both parameters are, however, not completely intuitive, i.e. in the case of POVPC local mobility is increased, while lateral diffusion is restricted, when comparing to the PGPC-containing bilayer. Linear fits to the diffusion times measured at different z-positions and plotted as a function of particle number have the y-intercept close to zero (data not shown), which means that a free diffusion is observed and there is no sign of phase separation [23].

Simulations

Orientation of oxidized lipid molecules in a bilayer can be analyzed by plotting distributions of tilt angles of the sn-1 and sn-2 chains of OxPLs with respect to the membrane plane normal. Fig. 2 depicts the tilt angle probability distribution of oxidized lipids compared with that of POPC. Unoxidized sn-1 chains behave similarly to sn-1 chains of POPC, namely, they are oriented mostly towards the membrane interior with a relatively small deviation of tilt angles from the 180° value. As a matter of fact, in PGPC and POVPC they are even more strongly pointing toward the membrane interior (i.e., perpendicular to the bilayer) than in POPC. In contrast, the orientation of oxidized sn-2 chains is qualitatively different from that of the sn-2 chains in POPC. Oxidized chains of POVPC, each terminated by the neutral but polar aldehyde group, undergo reorientation which is evidenced by the tilt angle spread

between 0° and 180° with a strong diminishment in the 180° region. In other words, sn-2 chains of POVPC become mostly reoriented from the direction into the bilayer pertinent to pure POPC, pointing now in all directions, and even being able to stick out of the membrane surface. In the case of PGPC the reorientation of negatively charged sn-2 chains is even more radical, with most of the oxidized chains sticking out of the membrane surface and with their tilt angle being mostly between 0° (i.e., sticking out perpendicular) and 90°(i.e., being parallel to the bilayer). Analogous changes in chain orientation upon oxidation have been also observed in recent simulations of similar OxPLs [17, 18]. Reversing of the oxidized chains of both the lipids is important for biological recognition of oxidation by various receptors [31].

In the case of POPC+PGPC system the reversal of the orientation of the oxidized sn-2 chains has direct influence on membrane compactness, which is reflected in the values of the area per lipid. The membrane becomes more compact due to removal of sn-2 chains from its interior which causes the decrease of the area per lipid to a value of about 0.61 nm^2, whereas the area per lipid calculated for the pure POPC membrane is equal to about 0.66 nm^2. In the case of POVPC enriched bilayer the decrease of the area per lipid was not observed. This can be rationalized by taking into account the spread of orientations of sn-2 chains in POVPC molecules. Fully reversed chains cause compression of the membrane, but there is also a significant fraction of sn-2 chains oriented parallel to the membrane surface which, in contrast, contribute to the surface area expansion. In the particular case of POPC + 10% POVPC these two factors tend to cancel out, resulting in the unchanged area per lipid. It should be noted, that for anionic PGPC the presence of sodium cations which are attracted to the membrane is an additional factor which leads to an increase of the membrane stiffness as observed in previous simulations [18, 24]. A similar effect is expected to be operational in the experimental system where salt solutions of physiological strength were used in the measurements. Also, in biologically relevant systems the presence of electrolyte ions is

important and their influence will be taken into account in future simulations of charged oxidized membranes.

The reversal of the orientation of the oxidized sn-2 chains upon their oxidation can explain the increased local mobility observed in the SR experiment. Most of the chains of PGPC, and a significant fraction of them for POVPC move away from the region of the sn-1 carbonyls, where the fluorescent probes monitor an increase of fluidity. A significantly stronger increase of fluidity observed for POVPC than that for PGPC can be rationalized in terms of differences in hydration of these groups. Fig. 3 depicts the calculated electron density profiles which show a significantly deeper penetration of water molecules into the POVPC-containing membrane than in the system with PGPC. Similarly, the calculated hydration levels depicted in Fig. 4 show that both the sn-1 carbonyl and headgroup hydration of POPC+POVPC prevails over that of POPC+PGPC. These calculations are in agreement with the headgroup hydration measured with SR method (Table 1). The lower hydration of PGPC-containing membrane can be understood taking into account the increased packing of lipids in this membranes as reflected in the above discussed areas per lipid results.

In order to understand the difference of lipid lateral diffusion observed experimentally for the membranes containing PGPC and POVPC one must again consider the orientation of sn-2 chains. Oxidized chains of POVPC with tilt angle values around 90° are able to interact with neighboring lipid molecules. Such interactions contribute to the hindering of lateral diffusion of lipids, even the local mobility at the glycerol level is not affected. In the case of PGPC the interactions of sn-2 chains with neighboring lipids are less relevant since the majority of oxidized chains are sticking out of the membrane.

Conclusions

In this paper, we presented results of SR and z-scan FCS measurements of hydration, local mobility, and lipid lateral diffusion in POPC bilayer containing 10 mol% of either PGPC or POVPC, complemented by atomistic-scale molecular dynamics simulations of the same systems. The combination of these methods allows interpretation of the observed complex effects at the detailed molecular level. Both experiments and simulations show that even a modest addition (10%) of OxPLs changes the structural properties of the bilayers, which leads to increased membrane fluidity, i.e., both the local headgroup mobility and the lateral diffusion is increased. Moreover, these changes depend on the chemical nature of the oxidized chains.

The terminal carboxylic groups (PGPC), which tend to orient into the aqueous solution influence the lipid lateral diffusion stronger than local mobility. In contrast, the chains terminated with aldehydic group (POVPC) acquire all orientations including that parallel to the bilayer, which affects local mobility more than lateral diffusion.

Acknowledgement

We are grateful to the Czech Science Foundation (EUROMEMBRANES project MEM/09/E006) and to the Czech Ministry of Education (grant LC512 to P.J. and LC06063 to M.H.) for support.

Figure Captions

Fig. 1. Chemical structures of POPC, PGPC, POVPC, Laurdan and Bodipy C12-HPC. The fluorophores are positioned in accordance with [21, 32].

Fig. 2. Tiltangle distributions of sn-1 and sn-2 chains in oxidized lipid molecules compared with those of the pure-POPC simulation. Tiltangle of 180° corresponds to a chain oriented in parallel to the membrane normal and pointing towards the membrane interior; 0° characterizes chains pointing towards water phase; 90° corresponds to a chain oriented perpendicular to the membrane normal. Angle histograms were divided by sin(angle) factor in order to get probability distribution of angles. Typical configurations observed for the three considered molecules are schematically depicted. The reversal of sn-2 chains of OxPLs is evident, for PGPC the effect is particularly strong as its titltangle distribution is concentrated mostly for <90°.

Fig. 3. Electron density distributions along the membrane normal calculated for either POPC or water molecules. The POPC density demonstrates that the thickness of both oxidized membranes is decreased with respect to the pure-POPC bilayer. For POPC+POVPC membrane a distinctive deeper water penetration is observed.

Fig. 4. Hydration levels calculated as average numbers of water molecules within 0.5 nm radius of each atom of either sn-1 carbonyl or headgroups for each simulated system. Hydration of both the sn-1 carbonyl and headgroup for POPC+POVPC prevails over that of POCP+PGPC (as shown also in Fig. 3).

Table 1. Fluorescence solvent relaxation parameters for Laurdan incorporated into bilayer consisted of POPC and oxidized phospholipids measured at 5°C and 10°C.

Lipid composition[a]	5°C			10°C		
	$\Delta\nu$ (cm^{-1})[b]	τ_r (ns)[c]	Observed[d]	$\Delta\nu$ (cm^{-1})[b]	τ_r (ns)[c]	Observed[d]
POPC	3750	4.05	89%	4000	3.30	86%
10% PGPC	3800	3.85	85%	4000	3.00	85%
10% POVPC	3900	3.55	86%	4050	2.85	87%

[a] Large unilamellar vesicles composed of either pure POPC or POPC with 10 mol% of one of oxidized lipids labeled with Laurdan (1:100)

[b] $\Delta\nu = \nu(0) - \nu(\infty)$, where $\nu(0)$ was estimated to be 23 800 cm^{-1}, and $\nu(\infty)$ was obtained by TRES reconstruction

[c] Integrated relaxation time: $\tau_r = \int_0^\infty C(t)dt$;

[d] Extent of the relaxation process captured by the instrumentation obtained by comparison of the $\Delta\nu$ value calculated using the $\nu(0)$ value from the time-zero estimation with that obtained by TRES reconstruction. Specifically, a value of 86% indicates that 14 % of the SR is occurring faster than the resolution of the experiment (i.e. 50 ps).

References

(1) Fruhwirth, G. O.; Loidl, A.; Hermetter, A. *Biochim. Biophys. Acta* **2007,** *1772*, 718–736.

(2) Watson, A. D.; Leitinger, N.; Navab, M.; Faull, K. F.; Horkko, S.; Witztum, J. L.; Palinski, W.; Schwenke, D.; Salomon, R. G.; Sha, W.; et al. *J. Biol. Chem.* **1997,** *272*, 13597–13607.

(3) Pidkovka, N.A.; Cherepanova, O. A.; Yoshida T.; et al. *Circ. Res.* **2007**, *101*, 792–801.

(4) Gago-Dominguez, M.; Castelao, J. E.; Pike, M. C.; Sevanian, A.; Haile, R. W. *Cancer Epidemiol. Biomarkers Prev.* **2005,** *14*, 2829–2839.

(5) Markesbery, W. R.; *Free Radic. Biol. Med.* **1997,** *23*, 134–147.

(6) Halliwell, B.; Gutteridge, J. M. *Methods Enzymol.* **1990,** *186*, 1–85.

(7) Deigner, H. P.; Hermetter, A. *Curr. Opin. Lipidol.* **2008**, 19, 289–294.

(8) Leitinger, N.; Tyner, T. R.; Oslund, L.; Rizza, C.; Subbanagounder, G.; Lee, H.; Shih, P. T.; Mackman, N.; Tigyi, G., Territo, M. C.; Berliner, J. A.; Vora, D. K. *Proc. Natl. Acad. Sci. U. S. A.* **1999**, *96,*12010 –12015.

(9) Johnstone, S. R.; Ross, J.; Rizzo, M. J.; Straub, A. C.; Lampe, P. D.; Leitinger, N.; Isakson B. E. *The American Journal of Pathology* **2009**, *175*, 916-924.

(10) Pegorier, S.; Stengel, D.; Durand, H.; et al. *Atherosclerosis* **2006**, *188*, 433–443.

(11) Smith, H. L.; Howland, M. C.; Szmodis, A.W.; Li, Q.; Daemen, L. L.; Parikh, A. N.; Majewski J. *J. Am. Chem. Soc.* **2009**, *131*, 3631–3638.

(12) Mason, R. P.; Walter, M. F.; Mason, P. E. *Free Radical Biology & Medicine* **1997**, *23*, 419–425.

(13) Erridge,C.; Kennedy, S.; Spickett, C. M.; Webb, D. J. *The Journal of Biological Chemistry* **2008,** *283*, 24748–24759.

(14) van Kuijk, F. J. K. M.; Sevanian, A.; Handelman, G. J.; Dratz, E. A. *Trends in Biochemical Sciences* **1987**, *12*, 31-34.

(15) Li, X. M.; Salomon, R. G.; Qin, J.; Hazen, S. L. *Biochemistry* **2007**, *46*, 5009–5017.

(16) Sabatini, K.; Mattila, J. P.; Megli, F. M.; Kinnunen, P. K.; *Biophys. J.* **2006**, *90*, 4488–4499.

(17) Wong-Ekkabut, J.; Xu, Z.; Triampo, W.; Tang, I-M.; Tieleman, D. P. *Biophys J.* **2007** *93*, 4225-4236.

(18) Khandelia, H.; Mouritsen, O. G.; *Biophysical J.* **2009**, *96*, 2734-2743.

(19) Cwiklik, L.; Jungwirth P. *Chem. Phys. Lett.*, **2010**, *486*, 99-103.

(20) Christova, Y.; James, P. S.; Jones, R. *Mol. Reprod. Dev.* **2004**, *68*, 365-372.

(21) Jurkiewicz, P.; Olzynska, A.; Langner, M.; Hof, M. *Langmuir* **2006** , *22*, 8741-8749.

(22) Jurkiewicz, P.; Sykora, J.; Olzynska, A.; Humplickova, J.; Hof, M. *Journal of Fluorescence* **2005,** *15*, 883-894.

(23) Machan, R.; Hof, submitted for publication.

(24) Vacha, R.; Siu S. W. I.; Petrov, M.; Bockmann, R. A.; Barucha-Kraszewska J.; Jurkiewicz, P.; Hof, M.; Berkowitz, M. L.; Jungwirth, P. *J. Phys. Chem. A* **2009**, *113*, 7235-7243.

(25) Hess, B.; Kutzner, C.; van der Spoel, D.; Lindhal, E. *J. Chem. Theory Comput.* 2008, 4, 435-447. GROMACS ver. 4. 0. 3, double precision compilation.

(26) Berger, O.; Edholm, O.; Jahnig, F. *Biophys. J.* **1997**, *72*, 2002-2013.

(27) Berendsen, H. J. C.; Postma, J. P. M.; van Gunsteren, W. F.; Hermans, J. In *Intermolecular Forces*; Pullman, B., Ed.; D. Reidel Publishing Company: Dordrecht, 1981; 331–342.

(28) Parrinello, M.; Rahman, A. *J. Appl. Phys.* **1981**, *52*, 7182-7190.

(29) Hoover, W. G. *Phys. Rev. A* **1985**, *31*, 1695-1697.

(30) Darden, T.; York, D.; Pedersen, L. *J. Chem. Phys.* **1993**, *98*, 10089-10092.

(31) Greenberg, M. E.; Li, X.; Gugiu, B.G.; et al. *J. Biol. Chem.* **2008**, *283*, 2385–2896.

(32) Šachl, R.; Boldyrev, I.; Molotkovsky J. G.; Johansson, L. B. A., submitted for publication.

Figure 1.

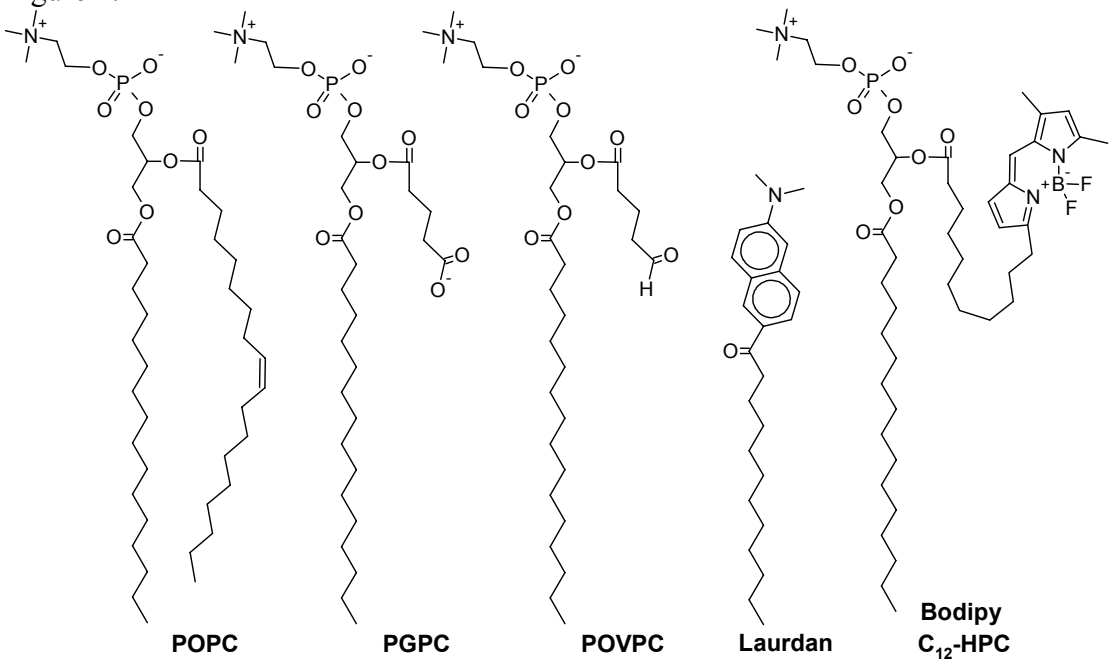

Figure 2.

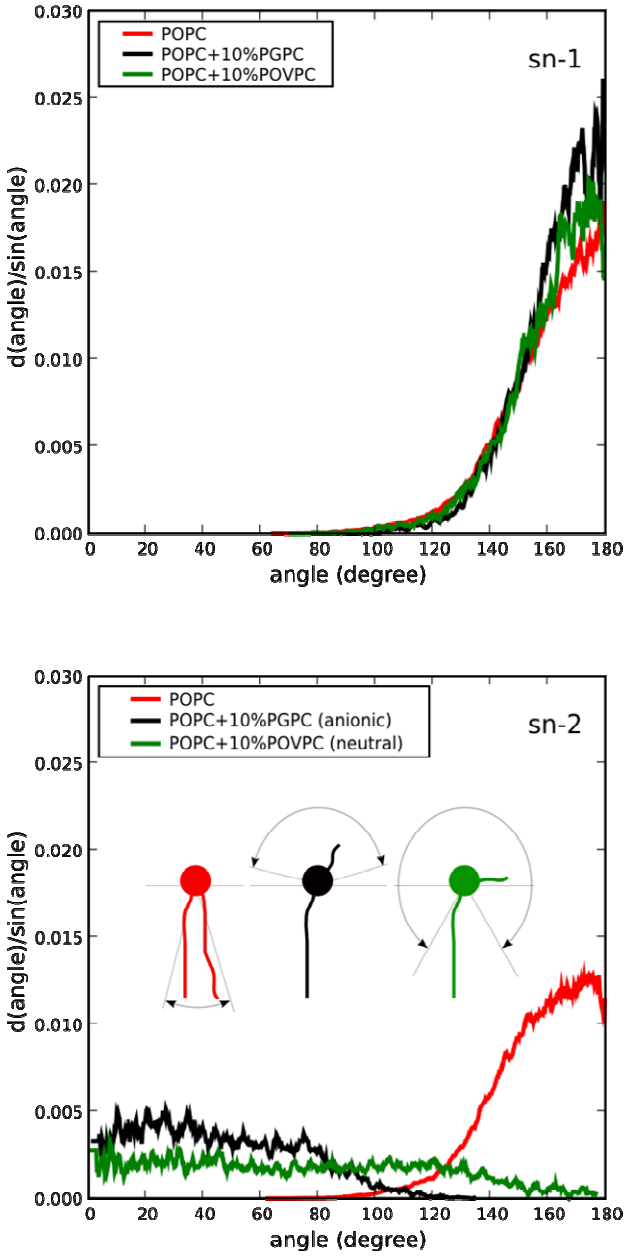
POPC
POPC+10%PGPC
POPC+10%POVPC
sn-1
d(angle)/sin(angle)
angle (degree)
POPC
POPC+10%PGPC (anionic)
POPC+10%POVPC (neutral)
sn-2
d(angle)/sin(angle)
angle (degree)

Figure 3.

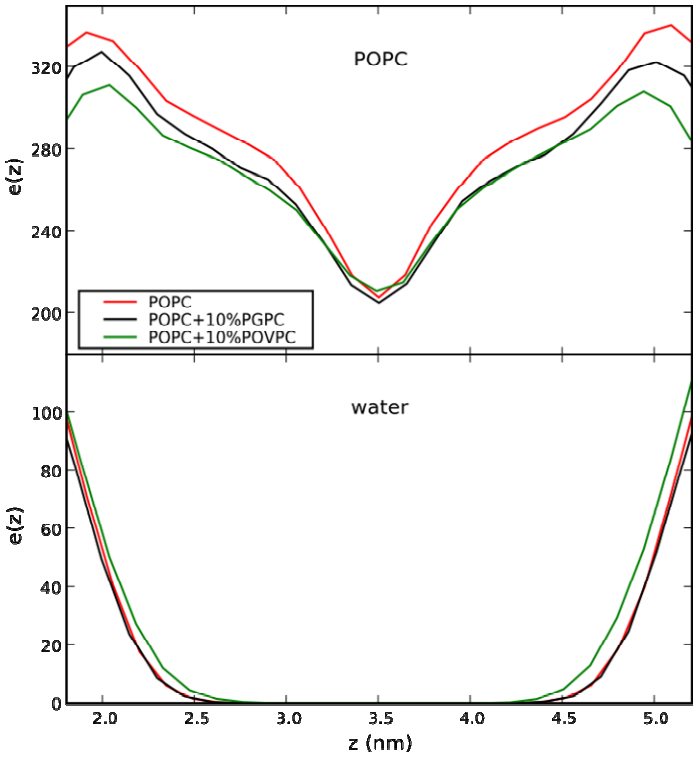
POPC
water
e(z)
e(z)
POPC
POPC+10%PGPC
POPC+10%POVPC
320
280
240
200
100
80
60
40
20
0
2.0
2.5
3.0
3.5
4.0
4.5
5.0
z (nm)

Figure 4.

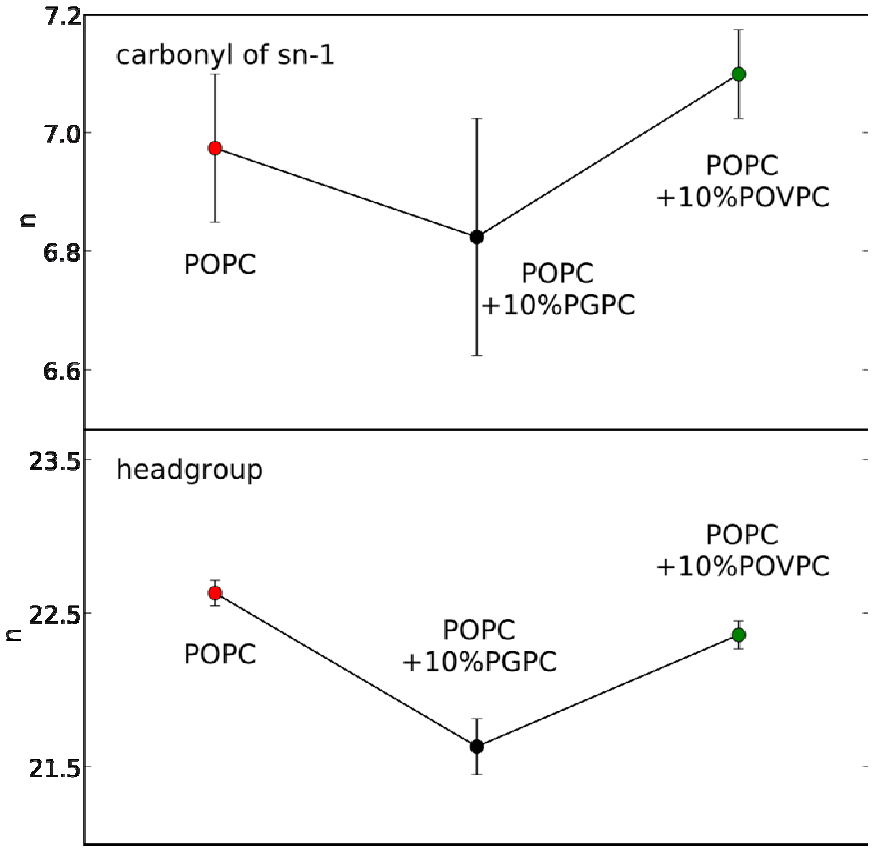
7.2
7.0
6.8
6.6
n
carbonyl of sn-1
POPC
POPC
+10%PGPC
POPC
+10%POVPC
23.5
22.5
21.5
n
headgroup
POPC
POPC
+10%PGPC
POPC
+10%POVPC